The Journal of Experimental Biology 216, 2789-2797

doi:10.1242/jeb.083352

RESEARCH ARTICLE

The hydrodynamics of contact of a marine larva, *Bugula neritina*, with a cylinder

Gregory Zilman[1,*], Julia Novak[1], Alex Liberzon[1], Shimrit Perkol-Finkel[1] and Yehuda Benayahu[2]

[1]School of Mechanical Engineering, Tel Aviv University, Tel Aviv 69978, Israel and [2]School of Life Sciences, Tel Aviv University, Tel Aviv 69978, Israel

*Author for correspondence (zilman@eng.tau.ac.il)

SUMMARY

Marine larvae are often considered as drifters that collide with larval collectors as passive particles. The trajectories of *Bugula neritina* larvae and of polystyrene beads were recorded in the velocity field of a vertical cylinder. The experiments illustrated that the trajectories of larvae and of beads may differ markedly. By considering a larva as a self-propelled mechanical microswimmer, a mathematical model of its motion in the two-dimensional velocity field of a long cylinder was formulated. Simulated larval trajectories were compared with experimental observations. We calculated the ratio η of the probability of contact of a microswimmer with a cylinder to the probability of contact of a passive particle with the cylinder. We found that depending on the ratio *S* of the swimming velocity of the microswimmer to the velocity of the ambient current, the probability of contact of a microswimmer with a collector may be orders of magnitude larger than the probability of contact of a passive particle with the cylinder: for *S*≈0.01, η≈1; for *S*≈0.1, η≈10; and for *S*≈1, η≈100.

Key words: larvae, *Bugula neritina*, settlement, hydrodynamics, trajectories, self-propulsion, microswimmer, contact probability, cylinder.

Received 3 December 2012; Accepted 28 March 2013

INTRODUCTION

Contact of a marine invertebrate larva with an underwater surface necessarily precedes its attachment to the surface. However, not all larvae that contact a substrate attach to it. Therefore, the probability of contact represents the upper bound of the probability of settlement. The probability of contact is a quantitative characteristic of settlement, which is of great interest in marine biology, particularly if attachment follows the first contact event (Abelson and Denny, 1997; Mullineaux and Butman, 1991; Mullineaux and Garland, 1993).

It is common to distinguish between the settlement of larvae on substrates of infinite extent and settlement on bodies of finite size. Because of the wide variety of larval forms and collector types, it is also common to observe settlement of specific larvae (e.g. bryozoan *Bugula neritina*) on relatively simple geometric forms, such as plates (Mullineaux and Butman, 1991; Mullineaux and Garland, 1993; Perkol-Finkel et al., 2008), cylinders (Harvey and Bourget, 1997; Rittschof et al., 2007) or inner sides of tubes (Crisp, 1955; Qian et al., 1999; Qian et al., 2000). Here, we studied the contact of *B. neritina* larvae with a long vertical cylindrical collector.

Most natural larval collectors are covered by microbial films (e.g. Dexter, 1979) or biofilms (e.g. Maki et al., 1989). The effect of microbial films and biofilms on bryozoan larval settlement has been observed both in the laboratory and under natural conditions (Brancato and Woollacott, 1982; Woollacott, 1984; Woollacott et al., 1989; Maki et al., 1989; Callow and Fletcher, 1995; Bryan et al., 1997). Generally, bryozoans are relatively indiscriminate settlers that may also settle on clean surfaces (Ryland, 1976; Dahms et al., 2004; Qian et al., 1999; Qian et al., 2000). We therefore used in our experiments a clean cylindrical collector that does not induce specific cues.

Chemical or physical cues play a central role in the behavioural biotic approach to larval settlement. In this approach a larva is attracted to a collector by cues and deliberately moves toward the collector. In an alternative mechanistic approach to larval settlement, a larva moves in the sea current as a drifter and collides with the collector as a passive particle. The issue of passive *versus* active contact has been intensively discussed in previous studies (Abelson et al., 1994; Butman, 1987; Butman et al., 1988; Harvey and Bourget, 1997; Harvey et al., 1995; Mullineaux and Butman, 1991; Mullineaux and Garland, 1993; Palmer et al., 2004).

However, the rich variety of models of larval contact with collectors cannot be described solely in terms of the antonyms ‘active–passive’. Consider, for instance, a realistic scenario of a swimming larva that is not aware of a collector. A swimming larva is active by definition, but in the absence of biotic factors influencing its contact with a collector, the larva moves as a mechanical object, i.e. as a microswimmer (e.g. Kirbøe, 2008). Nonetheless, the hydrodynamics and dynamics of such a microswimmer can be rather complex and difficult to describe in detail. Therefore, mathematical modelling of the motion of a larva as a mechanical object is inevitably associated with considerable simplifications, which should, however, retain the most relevant problem parameters, such as the Reynolds number of the cylinder (Re_c) and the Stokes number (St) of the particle–cylinder hydrodynamic system (Fuchs, 1964; Friedlander, 1977).

The Reynolds number $Re_c=\rho_f U_\infty D_c/\mu$ represents the ratio of the inertial and viscous forces acting on a cylinder. It depends on the fluid density ρ_f, its viscosity μ, the flow velocity far from the cylinder U_∞ and the diameter of the cylinder D_c. The Stokes number represents the ratio of inertial and viscous forces acting on a particle that moves in the velocity field of the cylinder. The Stokes number depends on the parameters that determine Re_c and additionally on the parameters that determine a particle’s inertia, its characteristic size d_p and its mean density ρ_p. A measure of the ratio of inertial

and viscous forces acting on a particle is its stopping distance, $l_p=\rho_p d^2_p U_\infty/18\mu$, the distance at which a particle that starts its motion in a stagnant fluid with speed U_∞ will be stopped by the drag force exerted on the particle by the fluid (Fuchs, 1964). The dimensionless Stokes number is the ratio of the stopping distance of a particle to the characteristic size of the collector, $St=l_p/D_c$ (Fuchs, 1964). Whereas the shape of a collector and its Reynolds number determine the collector's streamlines, the Stokes number characterises the degree of deviation of an inertial particle from the streamlines. The lower the Stokes number, the more a particle is 'embedded' in the fluid. Low-inertia particles (St<~0.1) follow streamlines rather closely and can be considered as inertialess particles, which follow streamlines exactly (Fuchs, 1964; Friedlander, 1977).

In contrast with passive particles, even an inertialess self-propelled microswimmer does not follow streamlines exactly. Zilman and colleagues (Zilman et al., 2008) theoretically studied the motion of a three-dimensional spherical microswimmer moving in a linear shear flow, in a channel flow and in a Poiseuille tube flow and calculated the probability of contact of the microswimmer with the walls bounding the flows. Crowdy and Samson (Crowdy and Samson, 2011) and Zöttl and Stark (Zöttl and Stark, 2012) studied trajectories of a two-dimensional and three-dimensional microswimmer moving in linear and Poiseuille shear flows, and took into account not only the re-orientation effect reported by Zilman and colleagues (Zilman et al., 2008) but also the direct hydrodynamic interaction of the microswimmer with a plane substrate.

In this work, we considered a previously unstudied problem, the motion of a low-inertia microswimmer (St<<1) in the velocity field of a large cylinder ($Re_c=10^2$–10^5). The aim of our study was to clarify how self-propulsion may influence the probability of contact of a microswimmer with a cylinder that does not induce biotic cues.

We observed the motion of *B. neritina* larvae in the velocity field of a cylinder and formulated a mathematical model of motion of a larva–microswimmer near the cylinder. We parameterised this mathematical model using experimental data, and calculated the probability of contact of larvae with a cylinder for a wide range of realistic problem parameters.

MATERIALS AND METHODS

We collected sexually mature colonies of *B. neritina* (Linnaeus 1758) from floating docks at the Tel-Aviv Marina in spring 2011, 2012. Larvae of *B. neritina* were maintained in laboratory conditions as described elsewhere (Qian et al., 1999; Wendt, 2000). The shape of *B. neritina* larvae is close to a prolate spheroid, with a length-to-maximal-width ratio of approximately 1.1. Such a spheroid can be approximated by a sphere of volume equal to the volume of the larva of interest. The diameter of the equivalent sphere approximating *B. neritina* larva varies as d_p=200–350 μm (Kosman and Pernet, 2009; Wendt, 2000). The sinking velocity of an immobilised *B. neritina* larva is approximately V_t=1 mm s^{-1} (Koeugh and Black, 1996). Correspondingly, the ratio of the mean larva density ρ_p to the water density ρ_f is ρ_p/ρ_f=1.02–1.04.

The motion of *B. neritina* larvae was observed in a transparent experimental flow tank (Fig. 1). Larvae were gently pipetted into the tank, and their trajectories were recorded, both from above and from the side of the tank, using an Optronis (Kehl, Germany) video system with two synchronised digital video cameras (500 frames s^{-1} and 1280×1024 pixel sensors) equipped with Nikkor (Nikon, Tokyo, Japan) 60 mm/f2.8 or 100 mm/f2.8 macro lenses. The trajectories were digitised using the Matlab Image Processing Toolbox and an open source software package (http://physics.georgetown.edu/matlab).

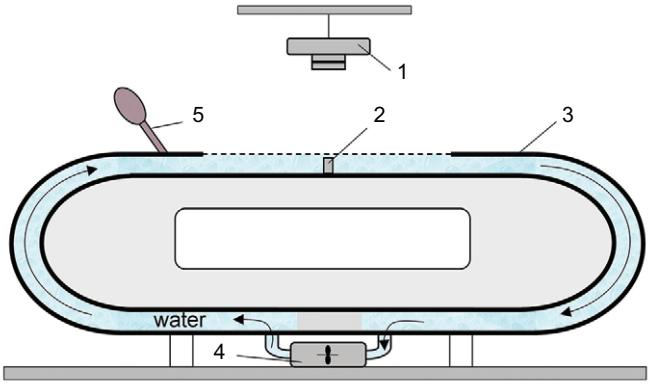

Fig. 1. The experimental setup (not to scale). (1) Top-view video camera; (2) cylinder; (3) flow tank; (4) water pump; (5) pipette with larvae. Transparent Plexiglas plates form a channel of length ~1.7 m, width 20 mm and height 40 mm. A Plexiglas cylinder of diameter D_c=10 mm and height 30 mm can be mounted in the middle of the channel. A solution of artificial seawater was circulated in the channel using a pump driven by an electric motor. The flow velocities were controlled in the range 1–6 cm s^{-1}.

The flow velocity in the experimental flow tank was measured using the particle image velocimetry system from TSI (Shoreview, MN, USA), which comprises a dual Nd:YAG laser Solo120XT (532 nm, 120 mJ pulse^{-1}, New Wave Research Inc., Fremont, CA, USA), a 4096×2048 pixel CCD camera with dynamic range 12 bits and a Nikkor 60 mm/f2.8 macro lens. Images were analysed using standard fast Fourier transform (FFT)-based cross-correlation algorithms and open-source software (http://www.openpiv.net) for verification purposes.

RESULTS

Experimental results

Tank without a cylinder

Typical trajectories of *B. neritina* larvae in still and moving water are shown in Fig. 2. In still water, a *B. neritina* larva moves for distances of the order of a few centimetres along a helix-like trajectory with an approximately straight axis but may also randomly change its direction of motion (Fig. 2A). The helical portions of a larva's trajectory can be approximated by a regular helix with a straight axis *ox* that points in the direction of the vector of the larva's swimming velocity $\mathbf{V}_S$. A larva moves along a helical trajectory with linear velocity $\mathbf{V}_h$ and rotates with angular velocity $\boldsymbol{\gamma}$.

In a Cartesian coordinate system, *oxyz*, the coordinates x_h, y_h, z_h of the centroid of a larva moving along a helical path vary with time t as $x_h=V_S t$, $y_h=0.5d_h\sin(\gamma t)$ and $z_h=0.5d_h\cos(\gamma t)$, where d_h is the diameter of the helix. The projections of the total velocity of a point of a helix $\mathbf{V}_h(t)$ on the axes of the coordinate system *oxyz* can be found as the time derivatives of the coordinates of the point of a helix, dx_h/dt, dy_h/dt and dz_h/dt, thereby yielding the relationship $V_S=\sqrt{(V_h^2-d_h^2\gamma^2/4)}$.

The diameter of the helix d_h and its temporary period T can be estimated experimentally, as illustrated in Fig. 2B. When a larva moves approximately horizontally, its swimming velocity V_S can be calculated directly. When the trajectory of a larva does not belong to the plane of a lens, Wendt (Wendt, 2000) suggested estimating V_h by filming the motion of the larva in a shallow depth of the field of the lens such that only a small portion of the trajectory is in focus. By calculating the velocity of a larva along this portion, one can estimate V_h.

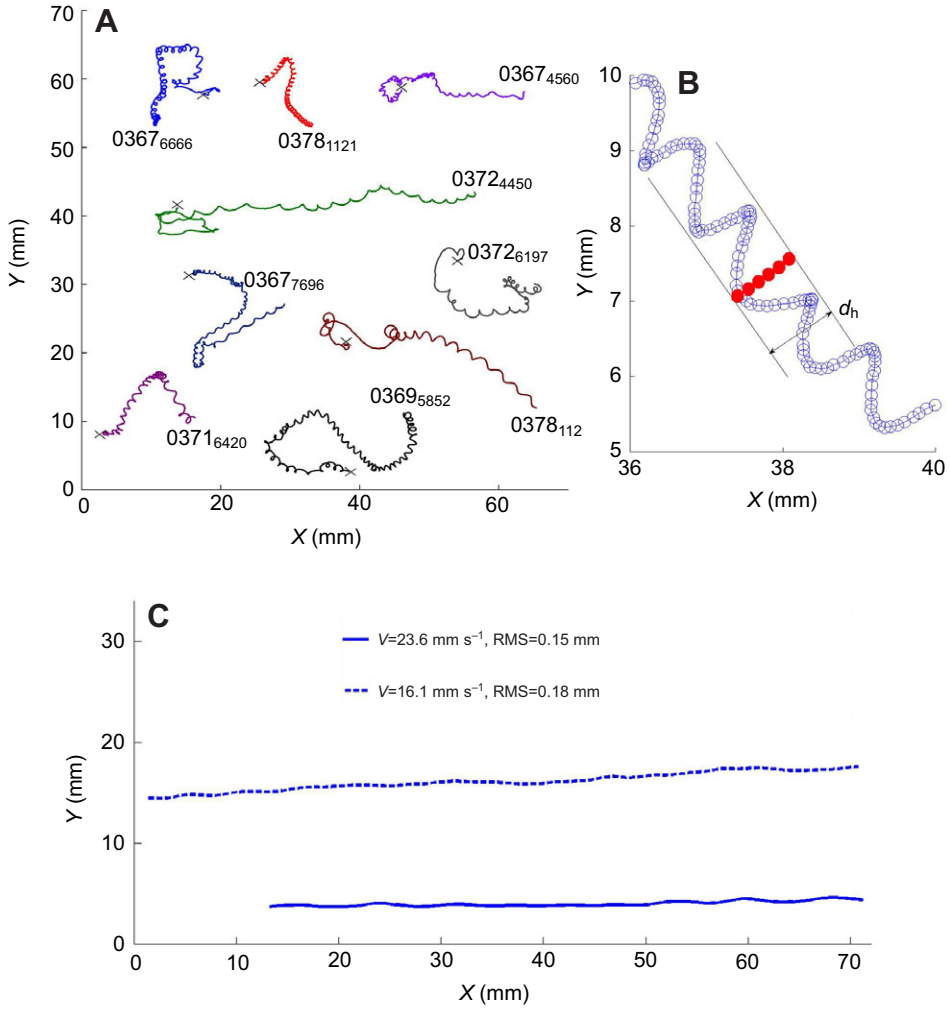

Fig. 2. Trajectories of larvae in a flume without a cylinder. (A) Still water. The cross denotes the beginning of the trajectory. Phototactile larvae biased their movements (from left to right in the figure) towards the illuminated side of the tank. (B) Enlarged part of trajectory 0369_{5852}. Open circles denote the consequent position of a larva at a resolution of 1/24 s. Filled red circles depict the estimated transverse displacement of larvae in the direction perpendicular to the direction of swimming measured in larval diameters. The radius of the diameter of a helix (d_h) can be estimated as approximately six larval diameters, the temporal period of the helix T can be estimated as ~1 s. The angular frequency of helical motion can be estimated as ~6.3 rad s^{-1}. (C) Motion of larvae in running water. The root mean square (RMS) deviation of the larva from a straight path is of the same order of magnitude as the deviation of a larva from the axis of a helix.

According to our measurements, $V_S \approx 3–6$ mm s^{-1}, which is consistent with Wendt (Wendt, 2000). Once V_S, d_h and $\gamma=2\pi/T$ are known, the projections of the velocity $\mathbf{V}_h$ on the axes of the coordinate system $oxyz$ can be found as time derivatives of the coordinates of the point of the helix dx_h/dt, dy_h/dt and dz_h/dt.

When a larva moves in a unidirectional flow for which the velocity is much greater than the larva's swimming velocity, the helical trajectory of the larva stretches, straightens and becomes rather close to rectilinear streamlines (Fig. 2C). Seemingly, in such a case, a larva moves as a passive particle. However, the contact problem relates to larval motion in non-uniform velocity fields of a collector, where streamlines are curvilinear and the fluid velocity may be of the same order of magnitude as the swimming velocity of a larva. In the next sections, we compare the motion of a larva and of a passive particle in the velocity field of a cylinder.

Tank with a cylinder

We studied trajectories of larvae, not the process of their attachment, because as stated in the Introduction, attachment depends on the physiochemical properties of the surface of a collector. Fig. 3A

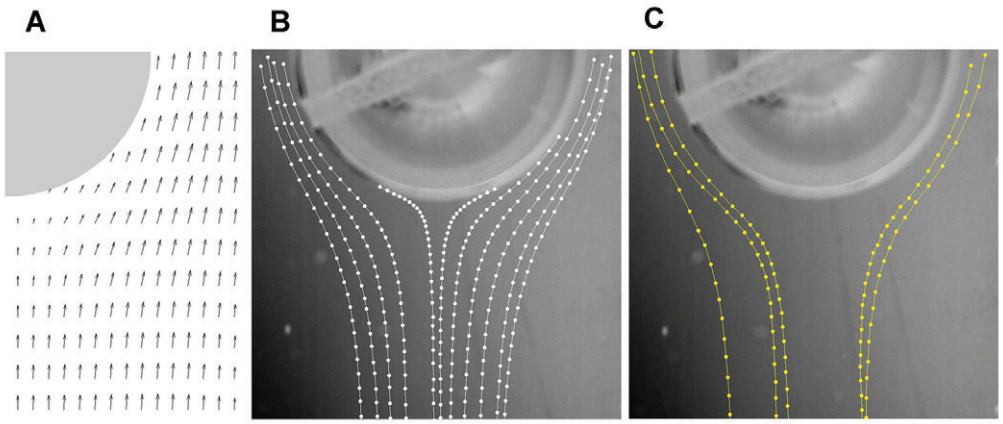

Fig. 3. Fluid velocity in a tank with a cylinder, and trajectories of beads and larvae (D_c=0.01 m, flow velocity far from the cylinder U_∞=0.03 m s^{-1}, Reynolds number of a cylinder Re_c=300). (A) Velocity field at the distance h_1=27 mm measured from the bottom of the flume. The velocity fields in the planes h_2=22 mm and h_3=15 mm are similar to those presented here. (B) Trajectories of spherical beads approaching the cylinder. (C) Trajectories of *Bugula neritina* in the velocity field of a cylinder, which are similar to the trajectories of beads.

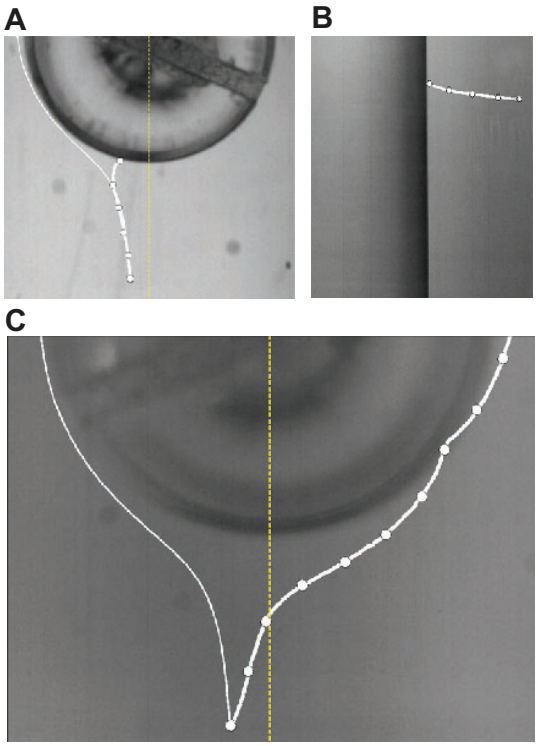

Fig. 4. Motion of a passive particle and a larva near a cylinder for the problem parameters given in Fig. 3. The lines with circular symbols indicate larvae. The lines without symbols indicate simulated trajectories of passive particles. (A,B) Trajectory of a larva with contact and attachment, viewed from above (A) and the side (B). After contact, the larva remains on the cylinder. (C) A larva approaches the cylinder closely but without attachment; the view is from above. A passive particle and a larva that start their motion at the same point move along different trajectories.

illustrates that the fluid velocity field in front of the cylinder is laminar and does not vary significantly between the horizontal planes h=15 mm and h=27 mm, where h is measured from the bottom of the channel. Spherical polystyrene beads of d_p=430 μm diameter and ρ_p=1.05 $\boldsymbol{g}$ cm^{-3} density were pipetted into the flow and allowed to circulate in the tank before settling on the bottom.

Fig. 3B shows typical trajectories of beads. A typical trajectory is characterised by smooth variation of its slope and smooth variation of its curvature; the latter changes the sign at a single inflection point of the trajectory. Using these criteria alone, one can infer that, on many occasions, larvae also move along typical trajectories (Fig. 3C). This similarity does not mean that a larva moves as a passive particle but only that the trajectory of a larva and that of a passive particle resemble one another as long as their slopes and curvatures vary in a similar manner.

However, in addition to the typical trajectories of larvae, we also observed a significant number of trajectories that we signify as atypical (n=23 in 560 tests) (Fig. 4). The atypical trajectories are characterised by an abrupt change in their slope at the points at which the distance between a larva and a cylinder's surface is minimal. No passive particle moves along such a trajectory. Thus, we suggest that atypical trajectories result from larval self-propulsion. Although the number of atypical trajectories is relatively small, they constitute the most salient qualitative manifestation of the influence of self-propulsion on larval trajectories in a non-uniform flow. Therefore, the atypical trajectories represent a considerable interest for our study. One of the aims of this work is to formulate a mathematical model of larval motion that is able to describe not only typical but also atypical trajectories.

A mathematical model of larval contact with a collector

A long vertical cylinder of diameter D_c is placed in an unbounded two-dimensional rectilinear current. The vector of current velocity $\mathbf{U}_\infty$ is normal to the cylinder's axis and lies in the horizontal plane. The Reynolds number of the cylinder varies between 10^2 and 10^5, which implies that the flow at the front part of the cylinder is laminar (Schlichting, 1979). For the further analysis we use the following assumptions. (1) There is no hydrodynamic interaction between individual larvae. (2) A larva is small compared with a collector and with the characteristic linear scale of the spatial flow variations that are induced by the collector in a uniform current. (3) A small larva does not change the velocity field of the cylinder. (4) The sinking velocity of a larva is small compared with the fluid velocity and can be disregarded in the problem of larval contact with the vertical surface of a cylinder. (5) A larva's relative velocity with respect to shear flow is equal to the larva's relative velocity with respect to the stagnant fluid. (6) The velocity field of the cylinder is two-dimensional; the vector of the fluid velocity $\mathbf{U}$ lies in the horizontal plane (Fig. 5). (7) The vector of a larva's swimming velocity ($\mathbf{V}_S$) is perpendicular to the axis of the cylinder and lies in the plane of flow (Fig. 5); the direction of $\mathbf{V}_S$ does not vary with respect to the rotating larva's body either in stagnant or in moving water. (8) In addition to an intrinsic self-induced rotation, a larva rotates as a small rigid sphere because of the shear-induced viscous torque.

Three primary mechanisms determine the collision of a passive particle: Brownian diffusion, inertial impaction and direct interception (Fuchs, 1964; Kirbøe, 2008). If the diameter of the particle d_p>>1 μm (which is always true for *B. neritina* larvae), Brownian diffusion does not influence the contact phenomenon under consideration (e.g. Kirbøe, 2008). The inertial impact is determined by the Stokes number of the problem. For the problem parameters adopted here, the Stokes number is much less than the threshold value 1/8, below which inertial impact of a spherical passive particle with a cylinder does not occur (Fuchs, 1964). Correspondingly, in our work, we consider only the mechanism of direct interception. Within the framework of this mechanism a larva follows the streamlines of a collector exactly and collides with the collector because of the larva's finite size.

For the subsequent analysis, we adopt a mathematic model of larval helical motion suggested by Brokaw and generalised by Crenshaw (Crenshaw, 1989), in which the vectors of a larva's swimming velocity $\mathbf{V}_S$ and of its angular velocity $\boldsymbol{\gamma}$ are collinear and are directed along the same axis ox (Fig. 5). Because the vector $\mathbf{V}_S$ lies in the horizontal plane, the vector $\boldsymbol{\gamma}$ is parallel to the horizontal plane. The vector of the angular velocity of the shear-induced rotation, $\boldsymbol{\omega}=2^{-1}\mathrm{rot}\mathbf{U}$ (Lamb, 1945), is perpendicular to vector of fluid velocity $\mathbf{U}$. For a two-dimensional horizontal flow, $\boldsymbol{\omega}$ is perpendicular to the horizontal plane and, thus, is perpendicular to $\boldsymbol{\gamma}$. The orthogonality of $\boldsymbol{\gamma}$ and $\boldsymbol{\omega}$ implies that shear-induced rotation of a larva does not change its intrinsic rotation about the axis ox.

In the earth-fixed frame of references, the direction of the larva's swimming velocity vector re-orients because of the larva's shear-induced rotation (Zilman et al., 2008). The re-orientation effect of a larva's motion in the shear flow of a cylinder is illustrated in Fig. 6. In the velocity field of a cylinder a larva moves along a curvilinear trajectory that cannot be described as a helix with a straight axis, i.e. as a regular helix. In this respect, the shear flow influences the helical pattern of motion.

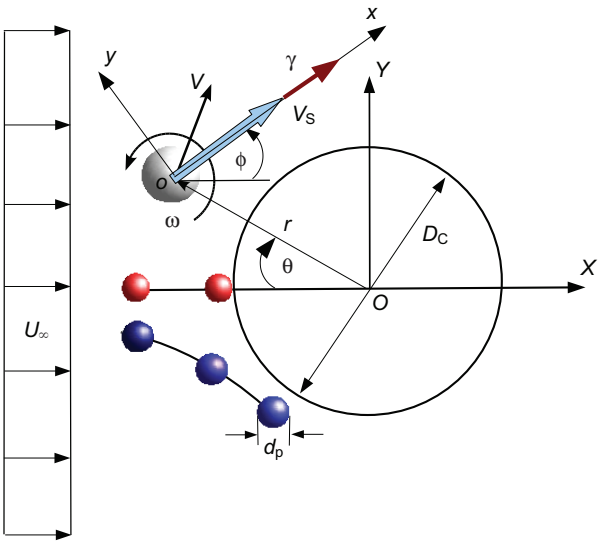

Fig. 5. Velocity field induced by the cylinder. The origin *O* of the cylinder-fixed coordinate system *OXYZ* coincides with the centre of the cylinder. The axis *OX* is collinear with the velocity vector $\mathbf{U}_\infty$. The coordinates of the centre of a microswimmer are defined by the radius vector **r**. The orthogonal coordinate system *oxyz* translates with the velocity of the centre of the microswimmer *V* and rotates with the shear-induced angular velocity ω. The vector of the swimming velocity $\mathbf{V}_S$ of the microswimmer is directed along the axis *ox* and constitutes with the axis *OX* the course angle ϕ. The vector angular velocity of the microswimmer **γ** is collinear with $\mathbf{V}_S$. Rotation of a spherical microswimmer about the axis *ox* does not influence the trajectory of the microswimmer in the plane *OXY*. The auxiliary polar angle θ=arctan(*Y*/*X*) is used here for calculating the velocity field around the cylinder. Outside the boundary, the fluid can be considered as inviscid and its motion as irrotational. Thus, the velocity field of a cylinder can be calculated as for a potential flow (Lamb, 1945). In the boundary layer, the fluid velocity component parallel to the contour of the cylinder is defined as $u_\theta=U(\theta)[F(\eta)+\Lambda(\theta)G(\eta)]$, where $U(\theta)$ is the fluid velocity at the contour of the boundary layer of thickness δ(θ), $F(\eta)$ and $G(\eta)$ are given polynomials of a non-dimensional coordinate $\eta=(r-D_c/2)/\delta$, and the tabulated values of δ(θ) and Λ(θ) are provided elsewhere (Schlichting, 1979). Once u_θ is known, the fluid velocity component v_r in the direction normal to the contour of the cylinder can then be obtained using the equation of mass conservation. Projecting (u_θ, v_r) onto the axes of the coordinate system *OXY*, we obtain **U** and $\boldsymbol{\omega}=2^{-1}\mathrm{rot}\mathbf{U}$, which are involved in Eqns 1 and 2.

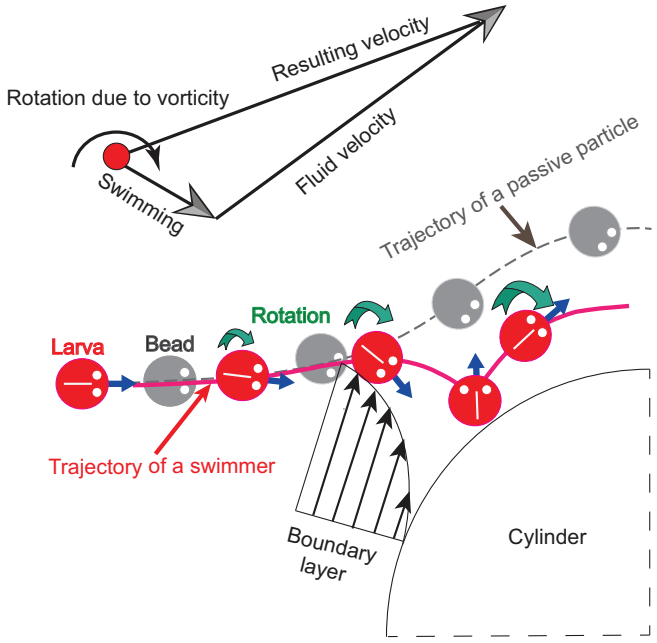

Fig. 6. Schematic trajectories of motion of a larva. Motion of a passive particle (grey symbols) and a microswimmer (red symbols) in the boundary layer of a collector. The linear velocity of a microswimmer is the geometrical sum of the flow velocity and the velocity of the swimmer. Because of translation, the microswimmer does not move along the trajectory of a passive particle. Additionally, both the microswimmer and the passive particle rotate as a result of boundary layer vorticity. The vector of the angular velocity of the shear-induced rotation is normal to the plane of the paper. For a spherical particle, the rotation does not influence its trajectory. A rotating microswimmer re-orientates and further deviates from the trajectory of a passive particle (Zilman et al., 2008). A small passive particle in the velocity field of a large collector moves along a streamline, which does not cross the cylinder. Deviation of a swimmer from the trajectory of a passive particle may result in its contact with the cylinder with much higher probability than the probability of contact with the cylinder of a passive particle.

To calculate the fluid velocity field near the front part of a cylinder, we use the boundary layer (BL) theory and von Kármán–Pohlhausen method, which is explained in detail elsewhere (Schlichting, 1979). In Fig. 5, we provide a brief description of this method.

In the cylinder-fixed Cartesian coordinate system *OXY* (Fig. 5), the linear velocity $\mathbf{V}=\mathbf{U}+\mathbf{V}_h$ of a massless swimmer can be represented as the time derivative of the radius vector of the centre of the swimmer $\mathbf{r}[X(t)Y(t)]$:

$$\frac{\mathrm{d}\mathbf{r}}{\mathrm{d}t}=\mathbf{V}(\mathbf{r})\,. \qquad (1)$$

The angular velocity of a larva ω about a vertical is equal to the time derivative of the track angle $\phi(t)$, the angle between the directions of the vectors **U** and $\mathbf{V}_S$ (Fig. 5):

$$\frac{\mathrm{d}\phi}{\mathrm{d}t}=\omega(\mathbf{r})\,. \qquad (2)$$

Eqns 1 and 2 determine the trajectory of a self-propelled larva–microswimmer in the two-dimensional velocity field of a collector. For prescribed initial conditions of a swimmer $X(0)=X_0$, $Y(0)=Y_0$ and $\phi(0)=\phi_0$, we solve the differential Eqns 1 and 2 numerically using the 4th-order Runge–Kutta method with an adaptive time step.

Theoretical results *versus* experimental observations

The degree of deviation of a microswimmer from the trajectory of a corresponding passive particle depends on the swimmer's velocity and on its initial conditions. Systematic numerical simulations show that depending on initial conditions, swimmers may move along typical or atypical trajectories. To calculate the trajectory of a microswimmer and compare it with an experimental trajectory of a larva, we must know the initial conditions of the larva's motion. Whereas the coordinates (X_0, Y_0) can be measured with high accuracy, measurement of the course angle ϕ_0 is difficult. Therefore, we compare the computed trajectories of a microswimmer with the experimental trajectories of a larva for the same measurable coordinates (X_0, Y_0) but for the track angle ϕ_0 estimated iteratively as a problem parameter (Eykhoff, 1974).

Similarities between the calculated trajectories of a microswimmer and the observed trajectories of larvae (Fig. 7) suggest that the main features of larval motion in the velocity field of a cylinder are faithfully captured by the mathematical model

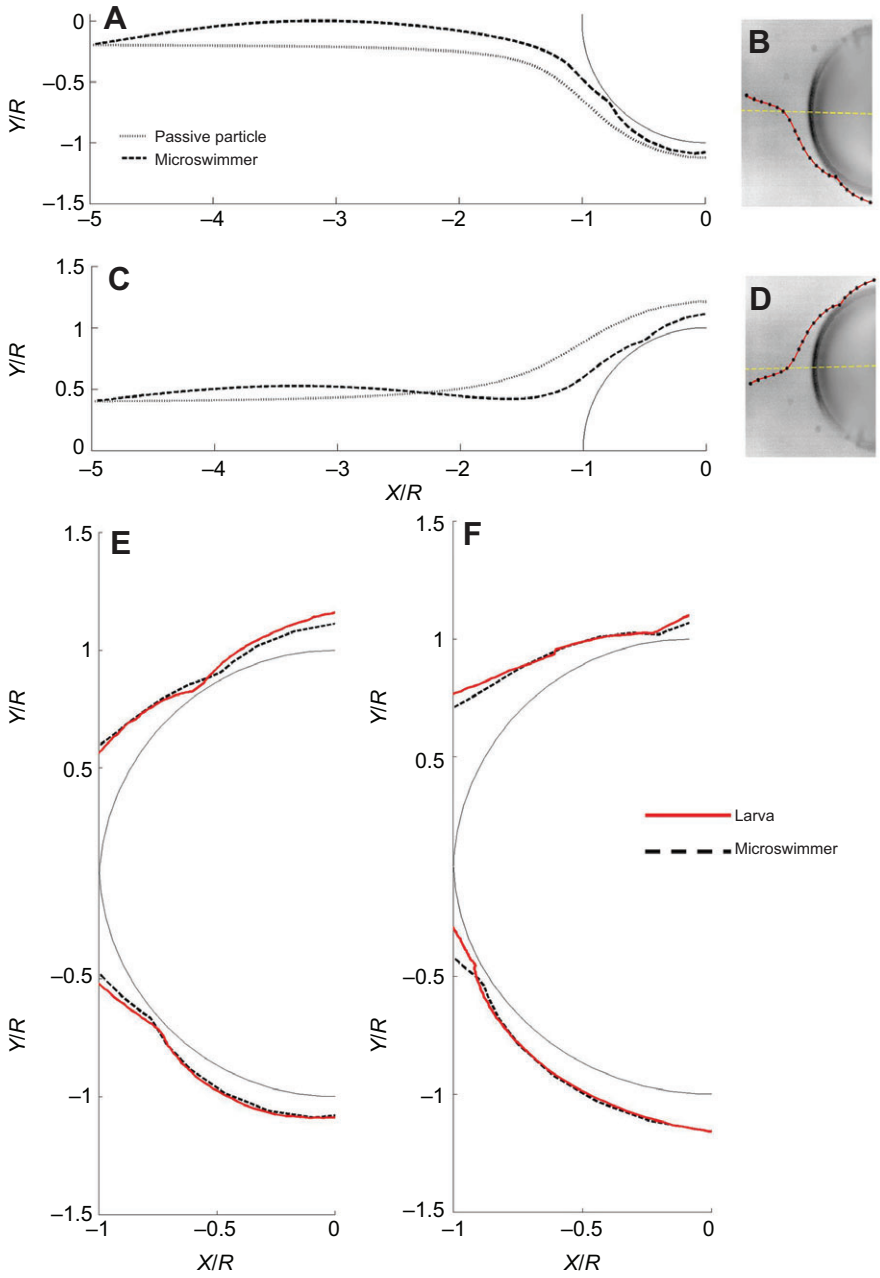

Fig. 7. Trajectories of a passive particle, microswimmer and larva near a cylindrical collector (D_c=0.01 m, d_p=250 μm, V_s=0.005 m s^{-1} and Re_c=300). The coordinates are normalised by the radius of the cylinder R (X_0/R=–5.0). (A) Modeled trajectories of a passive particle and of a microswimmer (Y_0/R=–0.2, ϕ_0=12.2 deg); (B) observed trajectory of a larva; (C) modeled trajectories of a passive particle and of a microswimmer (Y_0/R=0.4, ϕ_0=–10.2 deg); (D) observed trajectory of a larva; (E,F) qualitative comparison of experimental larval trajectories and modeled trajectories of microswimmers.

presented here. Although for each atypical trajectory the match between theoretical and experimental data was obtained for a particular initial angle ϕ_0 and a particular coordinate Y_0, the general character of atypical trajectories is determined by the local fluid mechanics in the closest vicinity of a collector, i.e. in its BL.

The trajectory of a larva defines a contact event. Thus, using the same mathematical model we can calculate the trajectory of a larva and the probability of its contact with a cylinder.

The probability of contact of a microswimmer with a collector

In the theory of aerosols (Fuchs, 1964), one of the methods of evaluating the probability of contact (collision) of passive particles with a collector (E_0), is based on the analysis of their trajectories. The trajectory analysis is applied here to calculate the probability of contact of a microswimmer with a collector (E_S). The mathematical details of the trajectory analysis are provided in Fig. 8. Satisfactory agreement between the theoretical and available experimental data of contact probability for passive particles, illustrated in Fig. 9, suggests that the mathematical model we used to calculate the contact probability of passive particles can also be used to calculate the contact probability of microswimmers.

Now, we return to the central question of our work: how does a larva's self-propulsion influence the probability of its contact with a collector if the larva is not aware of the collector? We characterise this influence as the ratio $\eta=E_S/E_0$, which is plotted in Fig. 10 for a wide range of realistic problem parameters adopted here.

DISCUSSION

Here, we observed trajectories of larvae *B. neritina* and of passive particles that mimic larvae in the velocity field of a vertical cylinder (Figs 3, 4). We revealed a considerable number of larval trajectories that differed markedly from the trajectories of passive particles (Fig. 4). We attributed such trajectories to larval self-propulsions. To explain our experimental observations, we formulated a

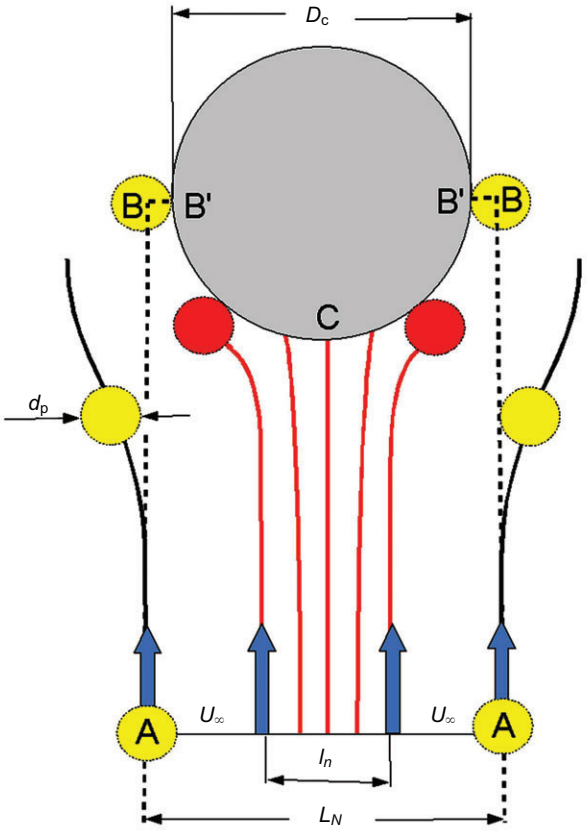

Fig. 8. Geometrical definition of the probability of contact (not to scale). The motion of particles (yellow circles) is tracked in the control volume ABB′CB′BA, which is fully penetrable except at the contour of the cylinder. Contact is assumed to occur if the distance from the centre of a particle to the cylinder is equal to the radius of the particle. Red lines and red circles represent the limiting (grazing) trajectories that for passive particles can be calculated iteratively, thereby yielding an estimate of the probability of contact $E_0=l_n/L_N$, where $L_N=D_c+d_p$ and l_n is the distance between the two limiting (grazing) trajectories. The method of grazing trajectories cannot be applied for swimmers because they start their motion with random angles of swimming. Instead, Monte Carlo simulations can be used as an alternative method of calculating of the probability of contact. It is possible to calculate the number of particles that contact the collector by tracking the trajectories of N particles that start their motion far from a cylinder with random uniformly distributed initial coordinates $-R<Y_0<R$ ($R=D_c/2$). The ratio of n particles that contact the cylinder to the total number of the particles N determines the probability of contact, $E_0=n/N$. To compare the probability of contact of passive particles E_0 with that of swimmers E_S, we must account for the randomness not only of the initial coordinate of the swimmer Y_0 but also of the initial track angle ϕ_0. Assume now that N_S microswimmers start their motion with random uniformly distributed coordinates $-R<Y_0<R$ and random uniformly distributed angles $0<\phi_0<2\pi$. Then, the ratio of n_S microswimmers that collide with the collector to the total number of the microswimmers N_S yields an estimate of the probability of contact of microswimmers, $E_S=n_S/N_S$ (Sobol, 1994). To obtain robust results, we repeated Monte Carlo simulations by doubling the number of testing points until the error of the estimate of the probability of contact was less than 5%. To obtain this degree of accuracy, we used $N_S\propto10^5$ test microswimmers.

mathematical model of a larva's motion in the two-dimensional laminar velocity field of a long cylinder ($10^2<Re_c<10^5$). The validity of our mathematical model was confirmed by satisfactory qualitative agreement between the experimental trajectories of larvae and the simulated trajectories of a microswimmer (Fig. 7) and by satisfactory quantitative agreement between simulated and

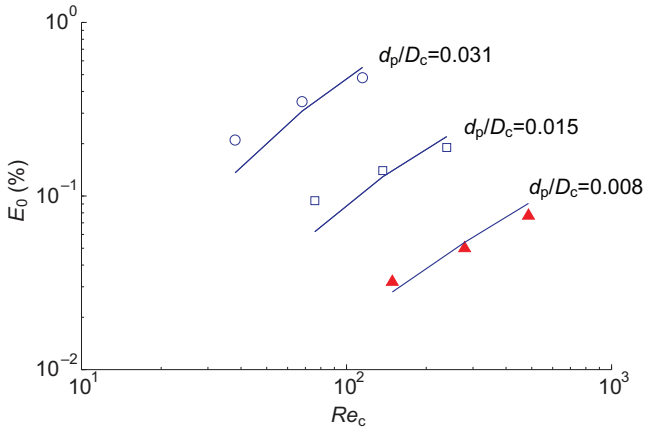

Fig. 9. Probability of contact of passive particles (d_p=194 μm). Solid lines are our numerical simulations. Symbols pertain to experimental values obtained by Palmer et al. (Palmer et al., 2004), who observed capture of spherical particles of diameter $d_p\approx194$ μm on a long vertical cylindrical of diameter of 0.63–2.54 cm in laminar flow (d_p/D_c=0.008 to 0.031, Re_c=68 to 486). The conditions of the Palmer et al. (Palmer et al., 2004) experiment match the assumption of our mathematical model. A discrepancy between the theoretical and experimental results can be observed in the range of Reynolds numbers less than 100, where the theory of the boundary layer is not expected to be accurate (Friedlander, 1977).

measured probabilities of contact of passive particles with a cylinder (Fig. 9).

Using trajectory analysis and Monte Carlo simulations, we calculated the probability of contact of a microswimmer with the front part of a cylinder. Mathematical modelling revealed a considerable increase in the probability of contact of the microswimmer with a cylinder compared with the probability of contact with the same cylinder of the same microswimmer but with zero swimming velocity, $\eta=E_S/E_0$ (Fig. 10). Regarding orders of magnitude, this increase can be estimated as follows: for $V_S/U_\infty\approx0.01$, $\eta\approx1$; for $V_S/U_\infty\approx0.1$, $\eta\approx10$; and for $V_S/U_\infty\approx1$, $\eta\approx10^2$. For instance, because of self-propulsion, larvae of *B. neritina* with

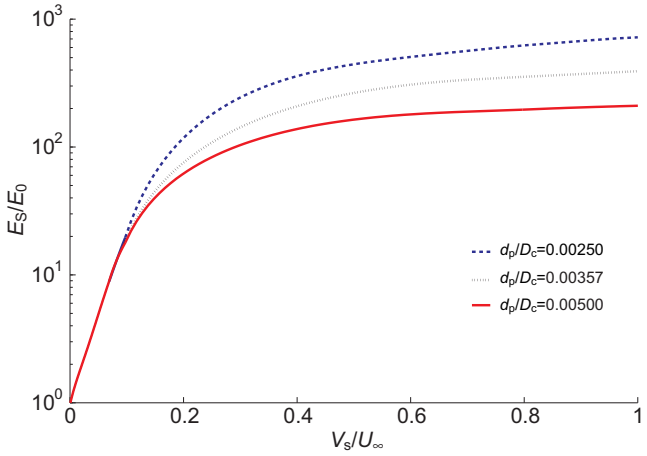

Fig. 10. Simulated probability of contact of microswimmers normalised by the probability of contact of passive particles (V_S=0.005 m s^{-1}, d_p=250 μm, $Re_c=2.5\times10^2$ to 10^4). In this figure the numerical simulations are performed for parameters of a regular helix $d_h=6d_p$, γ=6.3 rad s^{-1}. Systematic numerical simulations show that for $d_h=0$ the results presented here remain approximately the same. That implies that for the problem parameters presented here, the helical motion, including its irregularities, does not significantly affect the probability of contact.

Table 1. Fast larvae of marine invertebrates settling on protruding collectors

Taxon	Swimming speed ($cm\,s^{-1}$)	Source	Current velocity corresponding to η=10 $cm\,s^{-1}$ ($cm\,s^{-1}$)	Current velocity corresponding to η=100 $cm\,s^{-1}$ ($cm\,s^{-1}$)
Semibalanus balanoides	4.8–5.4	Crisp, 1955; Walker, 2004	68.5–77.1	24–27
Balanus crenatus	3.9	Crisp, 1955	55.7	19.5
Heterosaccus lunatus	1.8–2.8	Walker and Lester, 2000	25.7–40.0	9.0–14.0
Sacculina carcini	1.3–1.8	Walker and Lester, 2000	18.6–25.7	6.5–8.0
Hydroides elegans	1.5	Qian et al., 1999	21.4	7.5

η, normalised probability of contact of a larva with the collector.

swimming velocity ~5 $mm\,s^{-1}$ may increase their probability of contact with a cylinder 10-fold in a sea current of ~5 $cm\,s^{-1}$ and 100-fold in a sea current ~2.5 $cm\,s^{-1}$. Although sea currents of 2.5–5 $cm\,s^{-1}$ are rare, our theoretical prediction is consistent with the observations of Qian et al. (Qian et al., 1999; Qian et al., 2000): in tubes with laminar flow, larvae of *B. neritina* preferred to settle in low-speed currents $U\approx2.5\,cm\,s^{-1}$; whereas for $U>\sim8\,cm\,s^{-1}$, the probability of settlement drastically decreased. It should also be noted that some biofouling marine larvae swim much faster than larvae of *B. neritina* (Table 1). For those larvae, the ratio $V_S/U_\infty>0.1$, which provides a ~10- to 100-fold increase in the probability of contact, may correspond to frequent currents of the order of tens of $cm\,s^{-1}$ (Table 1). In contrast, within the framework of a mechanistic approach and according to the results of our mathematical modelling, larvae with $V_S<\sim2\,mm\,s^{-1}$ that move in sea current $U_\infty>5\,cm\,s^{-1}$ make contact with a collector as passive particles.

We formulated the problem of larval contact with a collector for a spherical microswimmer moving with low Reynolds numbers. However, such a small sphere and a small spheroid of moderate slenderness ~1.5–2.0 (such as the larvae listed in Table 1) move in a linear shear flow along similar trajectories (Zöttl and Stark, 2012). Given that a BL without separation can be approximated by a linear shear flow for qualitative estimates (Schlichting, 1979), it is not unlikely that a spheroidal swimmer may move in the two-dimensional BL approximately as a spherical swimmer.

We formulated the problem of contact of a microswimmer with a cylinder for laminar flows $Re_c>>1$. Experimental data regarding settlement (not contact specifically) of marine larvae on a cylinder in a natural turbulent environment were reported by Rittschof and colleagues (Rittschof et al., 2007). We did not find experimental or theoretical work in which the probability of contact of swimmers with a cylinder in turbulent flows was measured or calculated for $St<<1$ and $Re_c>>1$. For such flow parameters the available and rather limited experimental data pertain only to contact of passive particles with a cylinder. Asset and colleagues (Asset et al., 1970) and Stuempfle (Stuempfle, 1973) reported that for Stokes and Reynolds numbers such as those studied here, incoming upstream turbulence with an intensity of less than 7–8% practically does not affect the probability of contact of passive particles with a cylinder. In strong turbulence, the swimming speed of a larva may be small compared with the turbulent fluctuations of the fluid velocity. In such cases, a larva's self-propulsion may have little effect on its trajectory except in the vicinity of the collector, where the fluid velocity and its turbulent fluctuations are low (Schlichting, 1979).

The hydrodynamic model of contact of a microswimmer with a cylinder proposed here may be relevant for self-propelled larvae and aquatic larval collectors, such as kelp stems, sea grasses, small artificial reefs, pillars, columns and other engineering structures, that are located in a relatively slow sea current of low-to-moderate turbulent intensity (Abelson et al., 1994). Mathematical modelling of the motion of a larva in the velocity field of a collector located in a fully turbulent environment is beyond the scope of our present work.

In conclusion, the results of our investigation, which are presented in Fig. 10, suggest that for the problem parameters presented here, self-propulsion may greatly increase a larva's odds of making contact with the collector even if the larva does not detect the collector remotely.

LIST OF SYMBOLS AND ABBREVIATIONS

BL	boundary layer
D_c	diameter of a cylinder
d_h	diameter of a helix
d_p	equivalent diameter of a larva or particle
E_0	probability of contact of a particle with a collector
E_s	probability of contact of a microswimmer with a collector
l_n	distance between the two limiting (grazing) trajectories
l_p	the stopping distance a particle ($l_p=\rho_p d^2_p U_\infty/18\mu$)
n	number of particles that contact the cylinder
N	total number of particles used in Monte Carlo simulations
n_S	number of microswimmers contacting the cylinder
N_S	total number of microswimmers used in Monte Carlo simulations
oxyz	helix-fixed Cartesian frame of reference
OXYZ	earth-fixed Cartesian frame of reference
$\mathbf{r}$	radius vector of the centre of the particle
R	radius of a cylinder
Re_c	the Reynolds number of a cylinder ($Re_c=\rho_f U_\infty D_c/\mu$)
St	the Stokes number ($St=l_p/D_c$)
t	time
T	time period of a helix
$\mathbf{U}$	flow velocity
$\mathbf{U}_\infty$	flow velocity far from the collector
$\mathbf{V}$	velocity of motion of a larva or particle
$\mathbf{V}_h$	velocity of helical motion
$\mathbf{V}_S$	swimming velocity of a larva
V_t	sinking velocity of a larva
X_0, Y_0	initial coordinates of a larva or particle
γ	intrinsic angular velocity of a larva's helical motion
η	normalised probability of contact of a larva, E_S/E_0
μ	water viscosity
ρ_f	water density
ρ_p	mean density of a larva or particle
ϕ	course (track) angle of a larva
ϕ_0	initial course angle of a larva
ω	shear-induced angular velocity of a larva or particle

ACKNOWLEDGEMENTS

The authors are grateful to R. Strathman and M. Hadfield for constructive discussions. L. Kagan, J. Pechenic and L. Shemer read the manuscript and made many valuable comments. G. Gulitsky is acknowledged for the assistance in the design of the experimental flow tank and N. Paz for manuscript preparation.

AUTHOR CONTRIBUTIONS

All authors take full responsibility for the content of the paper and shared the writing and revising of the paper drafts. G.Z. conceived the main idea of the work,

formulated a mathematical model of contact of a microswimmer with a collector and together with Y.B. bridged this model with the biological content of the work. J.N. performed mathematical simulations, experiments and data analysis. A.L. focused on the flow measurements and revision of the paper drafts at final stages. S.P.-F. analysed the relevant biological literature, conceived the biological experiments, and together with J.N. performed biological experiments in the early stages of the research.

COMPETING INTERESTS

No competing interests declared.

FUNDING

This work was supported by the Israeli Science Foundation [research grant no. 1404/09].

REFERENCES

Abelson, A. and Denny, M. (1997). Settlement of marine organisms in flow. *Annu. Rev. Ecol. Syst.* **28**, 317-339.
Abelson, A., Weihs, D. and Loya, Y. (1994). Hydrodynamic impediments to settlement of marine propagules, and adhesive-filament solutions. *Limnol. Oceanogr.* **39**, 164-169.
Asset, G., Kimball, D. and Hoff, M. (1970). Small-particle collection efficiency of vertical cylinders in flows of low-intensity turbulence. *Am. Ind. Hyg. Assoc. J.* **31**, 331-334.
Brancato, M. S. and Woollacott, R. M. (1982). Effect of microbial films on settlement of bryozoan larvae (*Bugula simplex*, *B. stolonifera* and *B. turrita*). *Mar. Biol.* **71**, 51-56.
Bryan, J. P., Rittschof, D. and Qian, P.-Y. (1997). Settlement inhibition of bryozoan larvae by bacterial films and aqueous leachates. *Bull. Mar. Sci.* **61**, 849-857.
Butman, C. A. (1987). Larval settlement of soft-sediment invertebrates – the spatial scales of pattern explained by active habitat selection and the emerging role of hydrodynamical processes. *Oceanogr. Mar. Biol. Annu. Rev.* **25**, 113-165.
Butman, C. A., Grassle, J. P. and Webb, C. M. (1988). Substrate choices made by marine larvae settling in still water and in a flume flow. *Nature* **333**, 771-773.
Callow, E. M. and Fletcher, R. L. (1995). The influence of low surface energy materials on bioadhesion – a review. *Int. Biodeterior. Biodegradation* **34**, 333-348.
Crenshaw, H. C. (1989). Kinematics of helical motion of microorganisms capable of motion with four degrees of freedom. *Biophys. J.* **56**, 1029-1035.
Crisp, D. J. (1955). The behavior of barnacle cyprids in relation to water movement over a surface. *J. Exp. Biol.* **32**, 569-590.
Crowdy, D., Samson, O. (2011). Hydrodynamic bound states of a low-Reynolds-number swimmer near a gap in a wall. *J. Fluid Mech.* **667**, 309-335.
Dahms, H.-U., Dobretsov, S. and Qian, P.-Y. (2004). The effect of bacterial and diatom biofilms on the settlement of the bryozoan *Bugula neritina*. *J. Exp. Mar. Biol. Ecol.* **313**, 191-209.
Dexter, S. (1979). Influence of substratum critical surface tension on bacterial adhesion – *in situ* studies. *J. Colloid Interface Sci.* **70**, 346-354.
Eykhoff, P. (1974). *System Identification Parameter and State Estimation*. New York, NY: John Wiley.
Friedlander, S. K. (1977). *Smoke, Dust and Haze: Fundamentals Of Aerosol Behavior*. New York, NY: J. Wiley.
Fuchs, N. A. (1964). *The Mechanics of Aerosols*. Oxford: Pergamon Press.
Harvey, M. and Bourget, E. (1997). Recruitment of marine invertebrates onto arborescent epibenthic structures: active and passive processes acting at different spatial scales. *Mar. Ecol. Prog. Ser.* **153**, 203-215.
Harvey, M., Bourget, E. and Ingram, R. G. (1995). Experimental evidence of passive accumulation of marine bivalve larvae on filamentous epibenthic structures. *Limnol. Oceanogr.* **40**, 94-104.
Kirbøe, T. (2008). *A Mechanistic Approach to Plankton Ecology*. Princeton, NJ: Princeton University Press.
Koeugh, H. J. and Black, K. P. (1996). Predicting of scale of marine impact: understanding planktonic link between populations. In *Detecting Ecological Impact* (ed. R. Schmitt and C.W. Osenberg), pp. 199-234. San Diego, CA: Academic Press.
Kosman, E. T. and Pernet, B. (2009). Diel variation in the sizes of larvae of *Bugula neritina* in field populations. *Biol. Bull.* **216**, 85-93.
Lamb, H. (1945). *Hydrodynamics*. New York, NY: Dover Publications.
Maki, J. S., Rittschof, D., Schmidt, A. R., Snyder, A. G. and Mitchell, R. (1989). Factors controlling attachment of bryozoan larvae: a comparison of bacterial films and unfilmed surfaces. *Biol. Bull.* **177**, 295-302.
Mullineaux, L. S. and Butman, C. A. (1991). Initial contact, exploration and attachment of barnacle (*Balanus amphitrite*) cyprids settling in flow. *Mar. Biol.* **110**, 93-103.
Mullineaux, L. S. and Garland, E. D. (1993). Larval recruitment in response to manipulated field flows. *Mar. Biol.* **116**, 667-683.
Palmer, M. R., Nepf, H. M. and Pettersson, T. J. R. (2004). Observations of particle capture on a cylindrical collector: Implications for particle accumulation and removal in aquatic systems. *Limnol. Oceanogr.* **49**, 76-85.
Perkol-Finkel, S., Zilman, G., Sella, I., Miloh, T. and Benayahu, Y. (2008). Floating and fixed artificial habitats: spatial and temporal patterns of benthic communities in a coral reef environment. *Estuar. Coast. Shelf Sci.* **77**, 491-500.
Qian, P.-Y., Rittschof, D., Sreedhar, B. and Chia, F. S. (1999). Macrofouling in unidirectional flow: miniature pipes as experimental models for studying the effects of hydrodynamics on invertebrate larval settlement. *Mar. Ecol. Prog. Ser.* **191**, 141-151.
Qian, P.-Y., Rittschof, D. and Sreedhar, B. (2000). Macrofouling in unidirectional flow: miniature pipes as experimental models for studying the interaction of flow and surface characteristics on the attachment of barnacle, bryozoan and polychaete larvae. *Mar. Ecol. Prog. Ser.* **207**, 109-121.
Rittschof, D., Sin, T. M., Teo, S. L. M. and Coutinho, R. (2007). Fouling in natural flows: cylinders and panels as collectors of particles and barnacle larvae. *J. Exp. Mar. Biol. Ecol.* **348**, 85-96.
Ryland, J. S. (1976). Physiology and ecology of marine bryozoans. *Adv. Mar. Biol.* **14**, 285-443.
Schlichting, H. (1979). *Boundary Layer Theory*. New York, NY: McGraw-Hill.
Sobol, I. (1994). *A Primer for the Monte-Carlo Method*. Florida: CRC LCC Press.
Stuempfle, A. K. (1973). *Impaction efficiency of cylindrical collectors in laminar and turbulent fluid flow. Part III. Experimental.* Edgewood arsenal technical report AD909457. Fort Belvoir, VA: Defense Technical Information Center.
Walker, G. (2004). Swimming speeds of the larval stages of the parazitic barnacle, *Heterosaccus lunatus* (Crustacea: Ciripedia: Rhizocephala). *J. Mar. Biol. Assoc. UK* **84**, 737-742.
Walker, G. and Lester, R. J. G. (2000). The cypris larvae of the parasitic barnacle *Heterosaccus lunatus* (Crustacea, Cirripedia, Rhizocephala): some laboratory observations. *J. Exp. Mar. Biol. Ecol.* **254**, 249-257.
Wendt, D. E. (2000). Energetics of larval swimming and metamorphosis in four species of *Bugula* (Bryozoa). *Biol. Bull.* **198**, 346-356.
Woollacott, R. M. (1984). Environmental factors in bryozoan settlement. In *Marine Biodeterioration: an Interdisciplinary Study* (ed. J. D. Costlow and R. C. Tipper), pp. 149-154. Annapolis, MD: Naval Institute Press.
Woollacott, R. M., Pechenik, J. A. and Imbalzano, K. M. (1989). Effects of duration of larval swimming period in early colony development in *Bugula stolonifera* (Bryozoa: Cheilostomata). *Mar. Biol.* **102**, 57-63.
Zilman, G., Novak, J. and Benayahu, Y. (2008). How do larvae attach to a solid in a laminar flow? *Mar. Biol.* **154**, 1-26.
Zöttl, A. and Stark, H. (2012). Nonlinear dynamics of a microswimmer in Poiseuille flow. *Phys. Rev. Lett.* **108**, 218104.